

Monte Carlo simulation of quantum Potts model

Chengxiang Ding,^{1,*} Yancheng Wang,² Youjin Deng,³ and Hui Shao^{4,5}

¹*School of Science and Engineering of Mathematics and Physics,
Anhui University of Technology, Maanshan 243002, China*

²*Beijing National Laboratory for Condensed Matter Physics,
and Institute of Physics, Chinese Academy of Sciences, Beijing 100190, China*

³*Hefei National Laboratory for Physical Sciences at Microscale, Department of Modern Physics,
University of Science and Technology of China, Hefei, 230027, China*

⁴*Beijing Computational Science Research Center, Beijing 100193, China*

⁵*Department of Physics, Boston University, 590 Commonwealth Avenue, Boston, Massachusetts 02215, USA*

(Dated: March 11, 2022)

Using Monte Carlo simulations in the frame of stochastic series expansion (SSE), we study the three-state quantum Potts model. The cluster algorithm we used is a direct generalization of that for the quantum Ising model. The simulations include the one dimensional and two dimensional ferromagnetic three-state quantum Potts model and the two dimensional antiferromagnetic three-state quantum Potts model. Our results show that the phase transition of the one dimensional ferromagnetic quantum Potts model belongs to the same universality class of the two dimensional classical Potts model, the two dimensional ferromagnetic quantum Potts model undergoes a first order transition, which is also in analogy to its classical correspondence. the phase transition of the antiferromagnetic quantum Potts model is continuous, whose universality class belongs to the three-dimensional classical XY model, owing to an ‘emergent’ $O(2)$ symmetry at the critical point, although its ordered phase breaks the Z_6 symmetry.

PACS numbers: 05.50.+q, 64.60.Cn, 64.60.Fr, 75.10.Hk

I. INTRODUCTION

The Potts model[1], as a generalization of the famous Ising model, plays an important role in the study of phase transition and critical phenomena, which shows a typical phase transition of symmetry breaking. This model is widely studied, including the ferromagnetic case and antiferromagnetic case. However, the research of the quantum version of the model, i.e., the quantum Potts model[2] is relatively few[3, 4]. This seems somewhat strange, comparing to the fact that the quantum version of the Ising model, namely the quantum Ising model or the transverse field Ising model, has been studied extensively[5–10].

The quantum phase transition of the one dimensional ferromagnetic quantum Potts model is well understood[2, 11], the critical point $g_c = 1$ for all q , and the universality class being same as the corresponding two dimensional classical Potts model, which is first order for $q > 4$ and continuous for $q \leq 4$. The two dimensional ferromagnetic quantum Potts model is studied by the infinite projected entangled-pair state (iPEPS) algorithm[3], showing that both the 3-state and 4-state ferromagnetic quantum Potts models undergo a first-order phase transition. This result is easy to understand, because their classical correspondence, namely the classical three dimensional 3-state and 4-state ferromagnetic Potts models, also undergo first-order phase transitions. For the antiferromagnetic quantum Potts model, to the best of our knowledge, the study is almost blank except the recent work on the mixed classical Potts model[12], which can be considered as the classical correspondence of it.

In this paper, we will study the quantum Potts model by the means of Monte Carlo simulations in the frame

of stochastic series expansion (SSE), using a cluster algorithm which is a direct generalization of the cluster algorithm for quantum Ising model. Our study include both the ferromagnetic case and antiferromagnetic case.

II. MODEL AND METHOD

The Hamiltonian of the quantum Potts model[2] can be written as

$$H = -J \sum_{\langle i,j \rangle} \sum_{k=1}^{q-1} \Omega_i^k \Omega_j^{q-k} - g \sum_i \sum_{k=1}^{q-1} \Gamma_i^k \quad (1)$$

where Ω and Γ are $q \times q$ matrices. Ω is a diagonal one,

$$\Omega = \begin{pmatrix} 1 & & & & \\ & \omega & & & \\ & & \omega^2 & & \\ & & & \ddots & \\ & & & & \omega^{q-1} \end{pmatrix}, \quad \omega = e^{\frac{2\pi i}{q}}, \quad (2)$$

and Γ is an off-diagonal one,

$$\Gamma = \begin{pmatrix} 0 & I_{q-1} \\ 1 & 0 \end{pmatrix}, \quad (3)$$

where I_{q-1} is a $(q-1) \times (q-1)$ identity matrix. This model is ferromagnetic for $J = 1$ or antiferromagnetic for $J = -1$. $g \geq 0$ is the strength of the transverse field. When $q = 2$ it reduces to the quantum Ising model.

The exponential of the partition function $Z = \text{Tr}\{\exp(-\beta H)\}$ in SSE method[13, 14] is written as a Taylor expansion

$$Z = \sum_{\alpha_0} \langle \alpha_0 | \sum_{n=0}^{\infty} \frac{\beta^n}{n!} (-H)^n | \alpha_0 \rangle \quad (4)$$

* dingcx@ahut.edu.cn

where $|\alpha_0\rangle = |\sigma_1, \sigma_2, \dots, \sigma_N\rangle$ is the standard spin basis. Then, by inserting a set of complete basis, the partition function is rewritten as

$$Z = \sum_{\{\alpha_p\}} \sum_{n=0}^{\infty} \frac{\beta^n}{n!} \prod_{p=0}^{n-1} \langle \alpha_p | (-H) | \alpha_{p+1} \rangle \quad (5)$$

with $\alpha_n = \alpha_0$.

In the next step, the Hamiltonian is written as a sum of elementary lattice operators

$$H = - \sum_t \sum_a H_{t,a} \quad (6)$$

the subscript t and a refer to the type and the position of the operators respectively. Therefore, the partition function can be written as

$$Z = \sum_{\{\alpha_p\}} \sum_{n=0}^{\infty} \sum_{S_n} \frac{\beta^n}{n!} \prod_{p=0}^{n-1} \langle \alpha_p | H_{t_p, a_p} | \alpha_{p+1} \rangle \quad (7)$$

with $S_n = [t_1, a_1], [t_2, a_2], \dots, [t_n, a_n]$ the sequence of operators. The Taylor expansion in (7) can be truncated at certain power M for facilitating the implementation of the updating scheme. If M is large enough, the truncation error should be completely negligible. After the truncation, the partition function is written as

$$Z = \sum_{\{\alpha_p\}} \sum_{S_M} \frac{\beta^n (M-n)!}{M!} \prod_{p=0}^{M-1} \langle \alpha_p | H_{t_p, a_p} | \alpha_{p+1} \rangle \quad (8)$$

The binomial coefficient $M!/(M-n)!n!$ comes from the random insertion of the $M-n$ unit operators (which is often called ‘vacant’ operator in SSE simulations), because $n \leq M$. (8) is the starting point of the SSE Monte Carlo simulation, it defines the ‘SSE configuration’ which consists of a sequence of states $|\alpha_p\rangle = |\sigma_1(p), \sigma_2(p), \dots, \sigma_N(p)\rangle$ with $p=0$ to M (with $|\alpha_0\rangle = |\alpha_M\rangle$) and operators, whose weight is

$$\frac{\beta^n (M-n)!}{M!} \prod_{p=0}^{M-1} \langle \alpha_p | H_{t_p, a_p} | \alpha_{p+1} \rangle, \quad (9)$$

Fig. 1 shows a typical SSE configuration. It should be noted that it is not necessary to store all the states in the propagation direction, the information of $|\alpha_0\rangle$ and the sequence of operators can generate all the states.

In the quantum Potts model, the local basis (spin states) can be chosen as the eigenstates of the diagonal matrix Ω , take the case of $q=3$ for example, the local spin states are

$$|1\rangle = \begin{pmatrix} 1 \\ 0 \\ 0 \end{pmatrix}, |2\rangle = \begin{pmatrix} 0 \\ 1 \\ 0 \end{pmatrix}, |3\rangle = \begin{pmatrix} 0 \\ 0 \\ 1 \end{pmatrix}, \quad (10)$$

and the local Hamiltonian $H_{t,a}$ includes the diagonal operator $K_{i,j} = J(\Omega_i \Omega_j^2 + \Omega_i^2 \Omega_j)$ and the off-diagonal operator (transverse field) $R_i = g(\Gamma_i + \Gamma_i^2)$. For facilitating the simulation, we further define a diagonal operator $Q_i = g$. This operator also shifts the energy of the system but does not change the substantial physical properties of the model. The ‘vertex’ for the SSE simulation can be defined based on the operator and the states of the

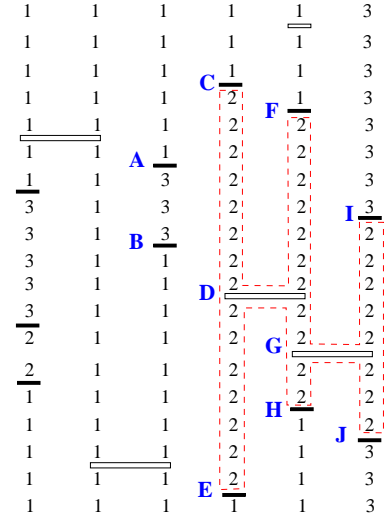


FIG. 1. A typical SSE configuration of the three-state quantum Potts model.

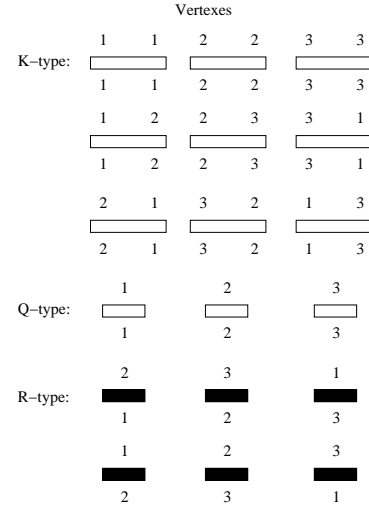


FIG. 2. SSE vertices of the three-state quantum Potts model. the K -type and Q -type vertexes are diagonal, the R -type vertex is off-diagonal.

spins connected to it, whose weight is $\langle \alpha_p | H_{t_p, a_p} | \alpha_{p+1} \rangle$. Corresponding to the operators, there are three types of vertexes, as shown in Fig. 2. The weight of the K -type vertex is

$$\langle \sigma_i, \sigma_j | K_{i,j} | \sigma_i, \sigma_j \rangle = J(-1 + q\delta_{\sigma_i, \sigma_j}). \quad (11)$$

When $\sigma_i \neq \sigma_j$, the weight is negative, which will lead to sign problem, thus in the simulations this weight is set as $C + J(-1 + q\delta_{\sigma_i, \sigma_j})$, which only shifts the energy of the system, but avoids the sign problem if the value of C is set properly. In the cluster algorithm that we will describe below, this value must be set as J for the ferromagnetic case ($J=1$) and $-J(q-1)$ for the antiferromagnetic case ($J=-1$). The weights of the R -type and Q -type vertexes are

$$\langle \sigma(p) | R | \sigma(p+1) \rangle = g(1 - \delta_{\sigma(p), \sigma(p+1)}), \quad (12)$$

$$\langle \sigma(p) | Q | \sigma(p+1) \rangle = g\delta_{\sigma(p), \sigma(p+1)}. \quad (13)$$

The weights of the two types of vertexes are complementary to each other, which allows a free change of the two

types of vertexes to each other in the procedure of simulation. This is very important for the realization of the off-diagonal update of the SSE configuration, including both the Metropolis algorithm and the cluster algorithm.

The simulation of Eq. (8) consists of the ‘diagonal update’ and ‘off-diagonal update’. For the diagonal update, the procedure consists of inserting a diagonal vertex to the sequence or removing a existing one. Both the K -type and Q type vertexes are diagonal, and the Metropolis procedure is performed as

1. if the vertex is vacant, the probability of trying to insert a K -type vertex is ξ , accordingly, the probability of trying to insert a Q -type vertex is $1 - \xi$. The acceptance probability of inserting the K -type vertex is

$$P = \frac{N_b \beta \langle \alpha_p | H_{t_p, a_p} | \alpha_{p+1} \rangle}{(M - n) \xi}. \quad (14)$$

Here N_b is the total number of bonds of the lattice. The acceptance probability of inserting a Q -type vertex is

$$P = \frac{N \beta g}{(M - n)(1 - \xi)}. \quad (15)$$

2. if the vertex is a diagonal one, then if it is K -type, the acceptance probability of removing it is

$$P = \frac{(M - n + 1) \xi}{N_b \beta \langle \alpha_p | H_{t_p, a_p} | \alpha_{p+1} \rangle}, \quad (16)$$

otherwise (it must be Q -type), the acceptance probability of removing it is

$$P = \frac{(M - n + 1)(1 - \xi)}{N \beta g}. \quad (17)$$

The selecting probability ξ can be adjusted to make the acceptance probability of inserting or removing to be a moderate one.

The off-diagonal update does not change the number of vertexes, but changes the type of vertexes. In hard-core boson or Heisenberg model or some other models, a loop algorithm is used, which is very efficient. For the quantum Potts model, two algorithms can be used for this purpose. The first one is a local updating algorithm (Metropolis), which is based on the fact that the change of the R -type vertex to Q -type vertex or conversely does not change the weight of the SSE configuration. For example, in Fig. 1 change of the state of the series of spins between the vertexes A and B (the state is $|3\rangle$) does not change the weight of the configuration; the state can be randomly given to be one of the q Potts states and the type of vertexes A and B should be changed from R -type to Q -type, if the state is changed to $|1\rangle$. Such algorithm is very easy to be implemented in compute programming.

However, the efficiency of the Metropolis algorithm is not satisfactory, especially for the large system at or near the critical point. which suffers from the problem of critical slowing down. Therefore the simulations call for a nonlocal algorithm. Such algorithm is available for our

model. In Ref. [15], a cluster algorithm is proposed for the quantum Ising model, which can be directly generalized to the quantum Potts model. In such algorithm, the construction of a cluster is started from a randomly selected leg of one vertex (not vacant), for example, a leg of a K -type vertex, then all the four legs and their links are considered to be in the same cluster and stored in the stack, then the links of the legs are used to be the new stating point (four branches) of the cluster constructing procedure. If the link is one of the leg of a R -type or Q -type operator, the constructing procedure terminates in such branch. The constructing procedure continues until all the possible branches terminates, then all the sates of spins of the cluster is flipped at the same time. For the quantum Potts model, the construction of the cluster is *exactly* the same as the quantum Ising model, but the spin state of the cluster is randomly set as one of the q Potts states; we also call this procedure as ‘flip’. As mentioned earlier, the const C is set as J for the ferromagnetic model, therefore the weights of the vertexes as shown in the second and third rows of Fig. 2 are zero, and the spins in the same cluster must have the same states. In the numerical procedure, one can construct all the clusters and flip every cluster with probability $1/2$ or construct *one* cluster and flip it with probability 1. The former is similar to the Swendsen-Wang algorithm[16] and the later is similar to the Wolff algorithm[17].

For the antiferromagnetic quantum Potts model, the diagonal update and the local algorithm for the off-diagonal update is the same as the ferromagnetic quantum Potts model, but the cluster algorithm have to be modified. Take the three-state Potts model for example, in the cluster constructing procedure, we can let the spins with state $|1\rangle$ be frozen, and the cluster is constructed for the spins with value $|2\rangle$ or $|3\rangle$. As mentioned earlier, the const C is set as $-J(q - 1)$, therefore the weights of the vertexes as shown in the first row of Fig. 2 are zero; every pair of spins at the same side of a K -type vertex must have different states. After the construction, the state of the spin in the cluster should be changed from $|2\rangle$ to $|3\rangle$ or conversely (flip). Sincerely, we can also froze the spins with state $|2\rangle$, and flip the spins with state $|1\rangle$ or $|3\rangle$; or froze $|3\rangle$, and flip $|1\rangle$ and $|2\rangle$. The ideal of such algorithm is very similar to the Wang-Swendsen-Kotecký algorithm[18] of the classical antiferromagnetic Potts model.

III. RESULT

A. ferromagnetic case

The temperature is set as $T = 1/L$, namely $\beta = L$. For the 3-state quantum Potts model, the simulated variables include the total energy E , the interaction energy E_z , the

the magnetization m , and the Binder ratio Q_m

$$E = -\frac{\langle n \rangle}{N\beta} + 2C + g \quad (18)$$

$$E_z = \left\langle \frac{1}{M} \sum_{p=0}^{M-1} E_z(p) \right\rangle \quad (19)$$

$$m = \langle |\mathcal{M}| \rangle = \left\langle \left| \frac{1}{M} \sum_{p=0}^{M-1} \mathcal{M}(p) \right| \right\rangle \quad (20)$$

$$Q_m = \frac{\langle \mathcal{M}^2 \rangle^2}{\langle \mathcal{M}^4 \rangle} \quad (21)$$

with

$$E_z(p) = \frac{-J}{N} \sum_{\langle i,j \rangle} (-1 + q\delta_{\sigma_i(p), \sigma_j(p)}) \quad (22)$$

$$\mathcal{M}(p) = \frac{1}{N} \sum_{i=1}^N \vec{\sigma}_i(p). \quad (23)$$

Here, the states of the spins has been mapped to two dimensional vectors by the rule $\vec{\sigma} = (\cos\theta, \sin\theta)$ with $\theta = 2\sigma\pi/3$. In (18), the const $2C + g$ is added to remove the energy shift that comes from the K -type and Q -type vertexes.

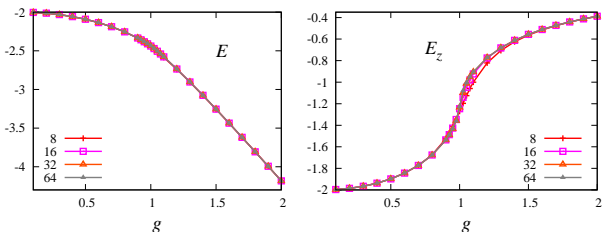


FIG. 3. Energy of the one dimensional three-state ferromagnetic quantum Potts model. Left, the total energy E ; right, the interaction energy E_z .

Firstly, we simulate the one dimensional three-state quantum Potts model to test the algorithm. The energy E and E_z are in shown in the Fig. 3. E is featureless while E_z obviously shows a phase transition. Such transition can also be detected by the magnetization m , as shown in the left of Fig. 4. In order to determine the critical point and critical exponents of the phase transition, we simulate the model near the critical point and fit the data of Q_m (as shown in the right of Fig. 4) with the finite-size scaling formula

$$Q_m = Q_c + \sum_{k=1}^2 a_k (g - g_c)^k L^{ky_t} + bL^{y_u}, \quad (24)$$

where g_c is the critical point, $y_t > 0$ the thermal exponent in the sense of renormalization, which is related to the critical exponent ν with $y_t = 1/\nu$; ν describes the divergence of the correlation length $\xi \sim |g - g_c|^{-\nu}$. y_u is the exponent of the irrelevant field in renormalization, which is negative; a_k and b are unknown parameters; Q_c is a shape-dependent universal parameter. The fitting gives $Q_c = 0.77(1)$, $g_c = 0.99999(1)$, and $y_t = 1.20(1)$. The estimated critical point and critical exponent coincides with the exact values[1, 2] $g_c = 1$ and $y_t = 6/5$.

Exactly at the critical point, the value of m scales with the system size with a power law formula

$$m = L^{y_h - d} (a + bL^{y_u}) \quad (25)$$

as shown in the subset of Fig. 4. Here, $y_h > 0$ is the magnetic exponent that describes the renormalization of the magnetic field; it is related to the exponent η with $y_h = 2 - \eta/2$; η describes the critical behavior of the correlation function $G(r) \sim r^{-\eta}$. The fitting gives $y_h = 1.876(5)$, which coincides with the exact one $y_h = 15/8$.

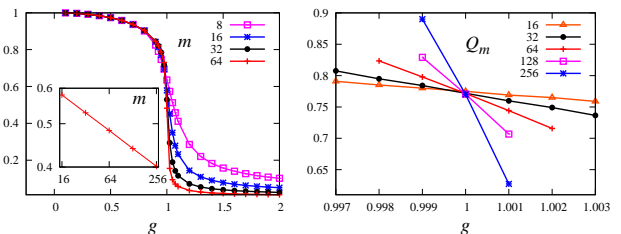


FIG. 4. The magnetization m and Binder ratio Q_m of the one dimensional three-state ferromagnetic quantum Potts model. The subset is the log-log plot of the magnetization m versus system size L with $g = g_c$.

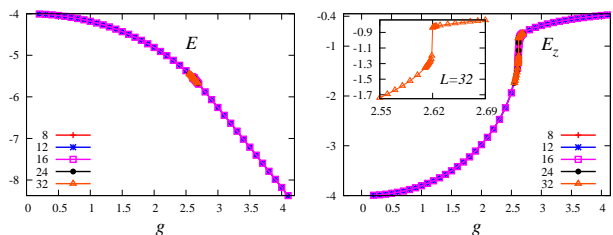


FIG. 5. Energy of the two dimensional three-state ferromagnetic quantum Potts model. Left, the total energy E ; right, the interaction energy E_z .

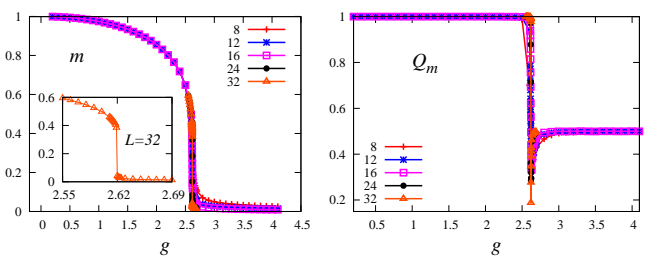


FIG. 6. Magnetization m and the Binder ratio Q_m of the two dimensional three-state ferromagnetic quantum Potts model.

Now we turn to the two dimensional model. The left of Fig. 5 shows the total energy of the three-state quantum Potts model on the square lattice, which does not show any singularity. However the interaction energy E_z shown in the right of Fig. 5 obviously show a gap, which is the typical feature of a first-order transition. Figure 6 shows the curves of m and Q_m versus g for a series of L , it also obviously shows the phase transition; the sharp falling of the magnetization the downward peak of the Binder ratio verifies that the transition is a first order one. From the behaviors of E_z , m , and Q_m , the transition point is estimated to be $g_c = 2.619(3)$.

B. antiferromagnetic case

We also simulate the antiferromagnetic quantum Potts model on the square lattice. In this case another order parameter called staggered magnetization is defined

$$m_s = \langle |\mathcal{M}_s| \rangle \quad (26)$$

with $\mathcal{M}_s = \mathcal{M}_A - \mathcal{M}_B$; \mathcal{M}_A and \mathcal{M}_B are defined by the similar way of (20), but confined to the sublattices A and B , respectively; a lattice site belongs to sublattice A or B according to the parity of $x + y$, with (x, y) the coordinate of the site. The Binder ratio of m_s is defined by the similar way of (21)

$$Q_s = \frac{\langle \mathcal{M}_s^2 \rangle^2}{\langle \mathcal{M}_s^4 \rangle} \quad (27)$$

The transition of the antiferromagnetic quantum Potts model is found to be continuous. The curves of the energy, the magnetization and the Binder ratio are similar to those of the one dimensional ferromagnetic quantum Potts model. The data of Q_s near the critical point can be fit by the formula (24), which gives $Q_c = 0.72(1)$, $g_c = 1.7173(3)$, and $y_t = 1.48(1)$. The value of y_t falls in the universality class of the three-dimensional classical XY model; to confirm this conclusion, we further simulate the model exactly at the critical point, and the data of m_s can also be fit with the ansatz (25). The fitting gives $y_h = 2.48(1)$, which is also consistent with the value of the three-dimensional classical XY model.

However, it should be noted that the symmetry of the ordered phase of the model (with small g) is Z_6 , which can be clearly demonstrated by the histogram of the staggered magnetization ($\mathcal{M}_{sx}, \mathcal{M}_{sy}$), as shown in Fig. 7(a). The Z_6 symmetry is not difficult to understand. In the ordered phase, an ideal ordered configuration may be: the spins on sublattice A take states $|1\rangle$, while the spins on the sublattice B randomly take states $|2\rangle$ or $|3\rangle$. There are six types of the such ideal states, owing to the permutation of the three states and the permutation of the two sublattices, therefore the symmetry of the order parameter is Z_6 . The XY universality class of the phase transition is owing to the ‘emergent’ $O(2)$ symmetry. Figure. 7(b) and (c) give the histograms with g slightly below and exactly at the critical point respectively, which obviously demonstrates the $O(2)$ symmetry.

The above results for the three-state quantum antiferromagnetic Potts model is very similar to the classical mixed Potts model[12] on simple cubic lattice, which can be considered as the classical correspondence of this model in the sense of universality.

IV. CONCLUSION AND DISCUSSION

In conclusion, we have studied the three-state quantum Potts model by Monte Carlo simulations in the frame of SSE; the cluster algorithm we used is a direct generalization of that for the quantum Ising model. The study includes the one and two dimensional ferromagnetic cases and the two dimensional antiferromagnetic case. The phase transition and critical phenomena are the same as the $d + 1$ dimensional classical Potts model in the sense of universality.

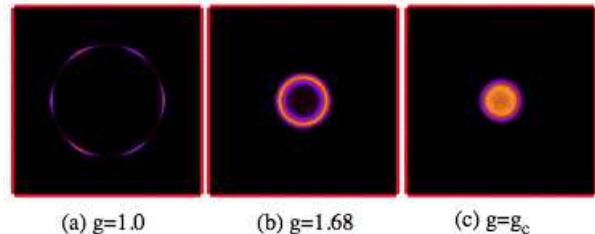


FIG. 7. Histograms of the staggered magnetization of the three-state antiferromagnetic quantum Potts model. The system size is $L = 24$.

The classical antiferromagnetic Potts model has very interesting phase transitions and critical phenomena[19–23], especially in two dimensions. Generally, the symmetry of the order parameter is determined not only by the symmetry of the Potts spin but also the lattice structure, for which the Z_6 and ‘emergent’ $O(2)$ symmetry is a good example; therefore the model may have different phases and phase transitions on different lattices for the same q . It is an interesting question if the quantum fluctuation is introduced for the antiferromagnetic Potts model. For example, in Ref. 12 the mixed Potts model with $q = 4, 5, \text{ and } 6$ are also studied, where an ‘emergent’ $O(n)$ symmetry is found, with $n = q - 1$. It is very possible that it is also the case for the antiferromagnetic quantum Potts model on the square lattice; we leave this question for further study.

V. ACKNOWLEDGEMENT

Ding is supported by the Anhui Provincial Natural Science Foundation under Grant Numbers 1508085QA05 and 1408085MA19. Deng is supported by the National Science Foundation of China (NSFC) under Grant Number 11625522.

-
- [1] F. Y. Wu, Rev. Mod. Phys. **54**, 235 (1982).
 - [2] J. Sólyom and P. Pfeuty, Phys. Rev. B **24**, 218 (1981).
 - [3] Y.-W. Dai, S. Y. Cho, M. T. Batchelor, and H.-Q. Zhou, Phys. Rev. E **89**, 062142 (2014).
 - [4] M. Campostrini, J. Nespolo, A. Pelissetto, and E. Vicari, Phys. Rev. E **91**, 052103 (2015).
 - [5] M. Powalski, K. Coester, R. Moessner, and K. P. Schmidt, Phys. Rev. B. **87**, 054404 (2013).

- [6] S. Wenzel, T. Coletta, S. E. Korshunov, and F. Mila, Phys. Rev. Lett. **109**, 187202 (2012).
- [7] S. E. Korshunov, Phys. Rev. B **86**, 014429 (2012).
- [8] S. V. Isakov and R. Moessner, Phys. Rev. B **68**, 104409 (2003).
- [9] L-P Henry and T. Roscilde, Phys. Rev. Lett. **113**, 027204 (2014).
- [10] S.-Z. Lin, Y. Kamiya, G.-W. Chern, and C. D. Batista, Phys. Rev. Lett. **112**, 155702 (2014).

- [11] R. J. Baxter, *J. Phys. C: Solid State Phys.* **6**, L1445 (1973).
- [12] C. Ding, H. W. J. Blöte, and Y. Deng, *Phys. Rev. B* **94**, 104402 (2016).
- [13] A. W. Sandvik and J. Kurkijärvi, *Phys. Rev. B* **43**, 5950 (1991).
- [14] A. W. Sandvik, *J. Phys. A* **25**, 3667 (1992).
- [15] A. W. Sandvik, *Phys. Rev. E* **68**, 056701 (2003).
- [16] R. H. Swendsen and J. S. Wang, *Phys. Rev. Lett.* **58**, 86 (1987).
- [17] U. Wolff, *Phys. Rev. Lett.* **62**, 361 (1989).
- [18] J. S. Wang, R. H. Swendsen, and R. Kotecký, *Phys. Rev. Lett.* **63**, 109 (1989).
- [19] M. Itakura, *Phys. Rev. B* **60**, 6558 (1999).
- [20] S.-Z. Lin, Y. Kamiya, G.-W. Chern, and C. D. Batista, *Phys. Rev. Lett.* **112**, 155702 (2014).
- [21] Y. Deng, Y. Huang, J. L. Jacobsen, J. Salas, and A. D. Sokal, *Phys. Rev. Lett.* **107**, 150601 (2011);
- [22] Q. N. Chen, M. P. Qin, J. Chen, Z. C. Wei, H. H. Zhao, B. Normand, and T. Xiang, *Phys. Rev. Lett.* **107**, 165701 (2011).
- [23] C.-X. Ding, W.-A. Guo, and Y. Deng, *Phys. Rev. B* **90**, 134420 (2014).